Modeling of a Low Voltage Cross-Coupled Oscillator

R. G. Ono[1], A. C. C. Telles[2]

rgono@cti.gov.br, antonio.telles@cti.gov.br

[1]Faculdade de Engenharia Elétrica
Pontifícia Universidade Católica de Campinas – Campinas/SP

[2]Division of Design, Analysis and Qualification of Electronic Circuits – DIPAQ
CTI Renato Archer – Campinas/SP

Abstract.

This work presents the analysis of the special case of the low-voltage cross-coupled oscillator when the transistors act as ideal switches. The motivation for developing it arises from the concept of Energy Harvesting, where the oscillator will serve to increase the input voltage. The primary objective is to achieve this goal with minimum use of components and space. A theoretical model, based on differential equations, is presented and compared to an experimental circuit. The work was carried out by building a circuit and measuring its parameters. The results demonstrated a very good agreement in the oscillation frequency, with the theoretical and experimental results showing a deviation of less than 2%.

1. Introduction

Autonomous systems like implanted sensors, wireless sensor networks and embedded systems require an energy source, usually in the form of a battery or supercapacitor. The miniaturization and reduction of power consumption in modern electronic devices enables using alternative energy sources as a way of extending the lifespan of these systems. The process of extracting and conditioning this energy is called usually as energy harvesting. The Internet of Things (IoT) is an especially favored area by the use of energy harvesting, due to the replacement of the batteries of the high number of devices involved. Some previous works analyzed the use of energy harvesting to feed IoT sensors [1, 2].

Some energy sources, such as single photovoltaic cells, are not able to feed directly the IoT sensors due to their low voltage output. One approach to harvesting energy of these low voltage sources is designing oscillators that can operate in these conditions.

One feasible configuration is the cross-coupled oscillator, which has extensive applications in the RF domain [3]. The cross-coupled oscillator was used in a circuit powered by a photovoltaic cell able to oscillate with a minimum voltage of 620 mV and deliver 1 mW from a supply of 700 mV [4].

The standard configuration includes a bias current at the transistor sources. The traditional method for analysis treats it as a linear circuit [3]. However, like all oscillators, the cross-coupled oscillator is inherently nonlinear.

Buonomo & Lo Schiavo examined the circuit as a VCO, with varactors controlling the frequency tuning [5, 6]. The analysis considered all nonlinearities, employing a hybrid approach combining the Poincaré-Lindstedt and Harmonic Balance methods, as developed by Buonomo & Di Bello [7].

The inclusion of the bias current source necessitates operation at higher voltages. When powered by photovoltaic cells, however, this voltage level is not available. Some researchers

have studied the oscillator without a bias current source. Ge et al. [8] explore the circuit's behavior under third-order nonlinearity. Daliri & Maymandi-Nejad [9] propose a model for a more generalized circuit, assuming that the output voltages are equal and phase-shifted by 180 degrees. Simulations are expected to yield an empirical value related to the crossing point of the drain waveforms. Machado et al. [10] modeled the oscillator using native transistors operating at ultra-low voltages with the small-signal approximation.

This study offers an analysis of a specific instance of the cross-coupled oscillator, operating without bias current and at low voltage levels. In the scenario examined, the transistors function as ideal switches, remaining in cutoff for half of the period.

A theoretical model was developed, based on differential equation modeling, and then compared to an experimental circuit. The practical aspect involved constructing the circuit and measuring its key parameters to validate the theoretical predictions. The core research question is whether the theoretical model accurately represents the real-world behavior of the circuit. This will be determined by analyzing the deviation between the theoretical model and the experimental results, with the accuracy of the modeling judged by how closely these deviations align.

2. Operation of the Cross-Coupled Oscillator

The proposed oscillator is depicted in Figure 1, with its operating principle outlined as follows. When M1 begins conducting at a specific moment, it results in a very small voltage drop between the drain and source, which in turn causes M2 to turn off. Consequently, the current through M2 abruptly halts, creating a negative current step in L2. Since M2 is cutoff, this current will flow through L2 and the parasitic components seen at drain of M2 (refer to Figure 2), resulting in a decaying sinusoidal voltage waveform at this point. This oscillation reinforces M1’s conduction.

In the same way, when the voltage at M2’s drain drops to zero, M1 turns off. This cessation of current at M1’s drain triggers oscillation at M2’s drain, which causes M2 to conduct and exhibits a minimal drop between its drain and source, leading to M1 turning off. M2 then replaces M1 in the cycle, completing the process.

Current and voltage waveforms are detailed in Section 4. For the circuit analysis, refer to Figure 2, where R1 and C1 are components connected to M2's gate, R2 and C2 are associated with M1’s drain, and r denotes the series resistance of the inductor.

The inductor and the equivalent resistance and capacitance form an RLC branch, for which the following differential equation defines the current:

$$V_{DD} - L\frac{di}{dt} - (R + r)i - \frac{1}{c}\int i\,dt = 0 \tag{1}$$

The initial conditions are the current through the transistor when it switches off and the voltage over the inductor and its equivalent resistance at this moment:

$$L\frac{di(0)}{dt} + ri(0) = V_{DD} \tag{1}$$

$$i(0) = I_M \tag{2}$$

Combining the initial conditions of (2) and (3) and using (1), one can prove that the current in this circuit is given by the formula:

$$i(t) = I_0 e^{-\sigma_0 t}\cos(\omega_D t + \theta_I) \tag{3}$$

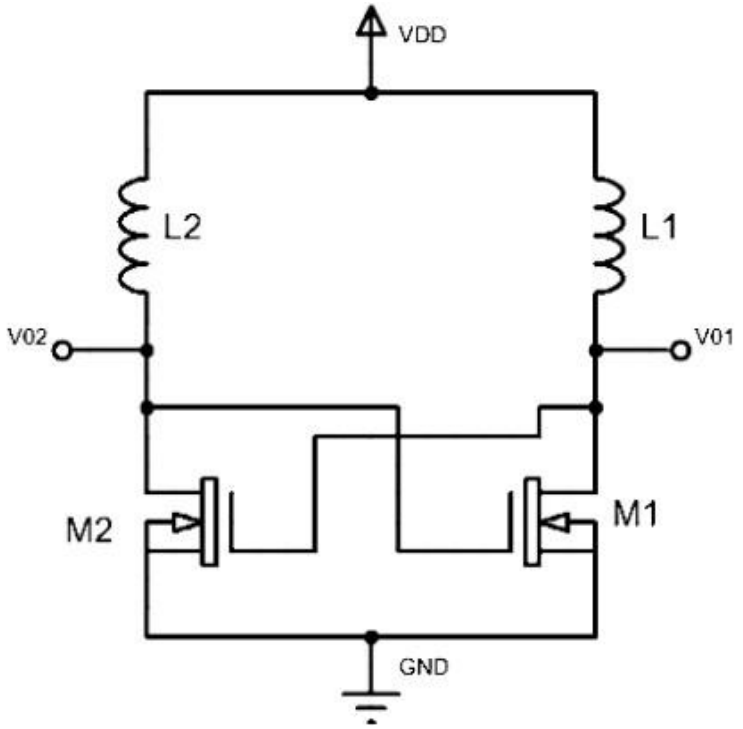

Figure 1. Schematic diagram of the oscillator

where:

$$\omega_D = \sqrt{{\omega_0}^2 - {\sigma_0}^2},\ \ \sigma_0 = \frac{R+r}{2L},\ \ \omega_0 = \frac{1}{\sqrt{LC}},$$

$$I_0 = \frac{I_M}{cos\theta_I},\ \ I_M = \frac{V_{DD}T_F}{2L},$$

$$\theta_I = tan^{-1}\left[-\left(\frac{2}{\omega_D T_F} + \frac{R-r}{2\omega_D L}\right)\right].$$

V_{DD} is the power supply, T_F is the period of oscillation, R and C are respectively the equivalent resistance and capacitance seen by the inductance. L1 and L2 are identical with the value of L. During the conduction of the transistor, the current is a ramp due to the integration of the constant voltage V_{DD} over the respective inductor. I_M is the peak current at the inductor, which occurs at the moment the transistor turns off (T_F/2).

According to Kirchhoff laws, the output voltage v_0 at the drain of any transistor is:

$$v_0(t) = V_{DD} - L\frac{di}{dt} - ri \tag{5}$$

Applying (4) on (5) and after some algebraic manipulation, one can prove that v_0 is given by the expression:

$$v_0 = V_{DD} + R_0 I_0 e^{-\sigma_0 t}[\sin(\omega_D t + \theta_I + \theta_D)] \tag{6}$$

where:

$$\theta_D = tan^{-1}\left(\frac{R-r}{2\omega_D L}\right),\ \ R_0 = \sqrt{\frac{L}{C} - Rr}.$$

Eq. (6) shows that v_0 is higher than V_{DD}, resulting in an amplification of the output voltage. The peak value of v_0 depends on R_0 and I_0. Mainly the relation L/C defines R_0. Once the parasitic capacitance is known, it is possible to define the inductance to a specified peak voltage. Parasitic resistances should be minimized with the same objective. I_0 is related to the peak current, which is inversely proportional to the inductance. Both results point out that the parasitic capacitance should be minimized in order to have the maximum peak voltage.

3. Experimental Setup

To perform the initial tests on the oscillator, the following measurement instruments were used:

- Waveform generator: Agilent 33250A
- DC power supply: Agilent E3631A
- Oscilloscope: Tektronix TDS 2014B
- LCR meter: Agilent E4980A
- Probes:
    - Tektronix CT-1 (current)
    - Tektronix P2220 (voltage)

Figure 2 illustrates how these parasitic elements are incorporated into the circuit. To determine the values of these elements (resistances and capacitances), a test was performed using the 33250A waveform generator, the oscilloscope with current and voltage probes and two MOSFETs to simulate the circuit. The values for R1, R2, C1, and C2 were obtained by measuring the voltage and current amplitudes and their phase differences. Figure 3 illustrates the circuit used for finding the parasitic components. In this circuit, an ammeter represents the current probe.

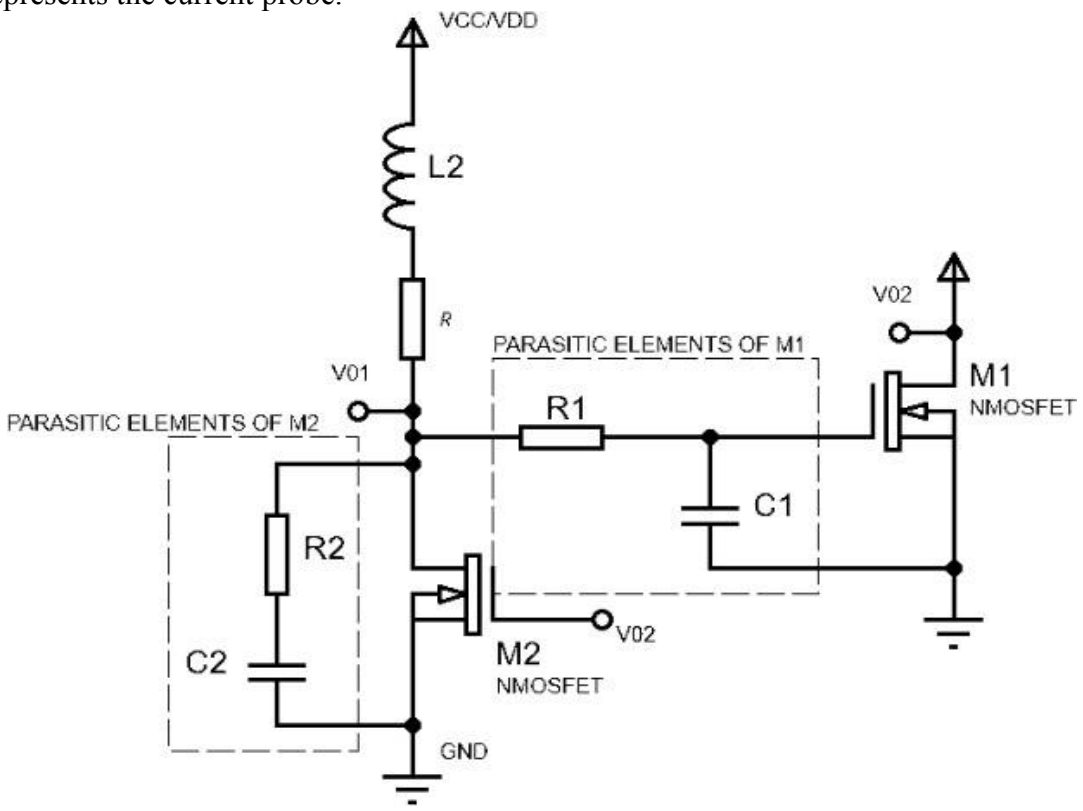

Figure 2. Parasitic elements in the circuit

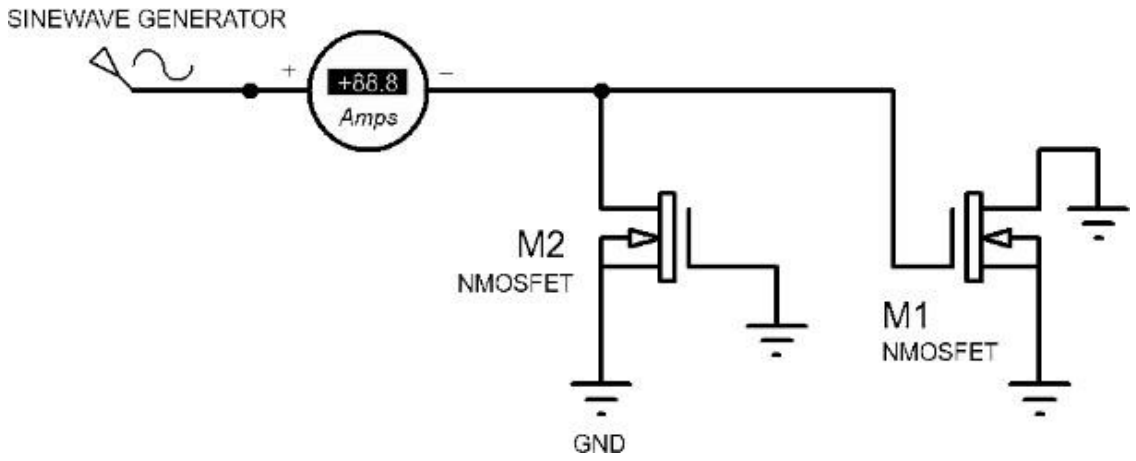

Figure 3. Circuit used to measure parasitic elements

To determine the resistance and inductance, the characterization of three inductors available for L1 and L2 was also made. For this, a protoboard and one inductor at a time were used, along with the E4980A RLC meter. The results obtained for the frequency of 2.0 MHz are shown in Table I. Therefore, it was possible to determine an average inductance and resistance of 3.30 μH and 290 mΩ respectively.

Table 1. Electrical parameters of the inductors

Parameter	Inductor 1	Inductor 2	Inductor 3
Inductance	3.28 μH	3.31 μH	3.32 μH
Resistance	230 mΩ	280 mΩ	360 mΩ

4. Experimental Results

The circuit was assembled using BSH103 transistors from NXP because of their high current capacity and low threshold voltage. Characterization of the parasitic components, as described previously, yielded the equivalent values of C = 731 pF and R = 18.0 Ω. The circuit begins oscillating when the voltage reaches 639 mV.

Current and voltage waveforms at a 2.0 V power supply are displayed in Figures 4, 5, and 6. The voltage waveforms closely resemble sinusoids, with each transistor reaching cutoff during half of the period.

A significant ringing is observed in the waveforms. This effect is caused by the approximation of the drain voltage to the threshold voltage V_{TH} (about 1.06 V for the BSH103). In this situation, when the waveform at the drain of one transistor, say M1, is getting close to V_{TH}, it starts to cut the current of the other one, M2. When this happens, the voltage at the drain of M2 starts to rise, leading M1 to rise its current and its drain voltage, since it is now in the weak to moderate inversion level.

The increase in the drain voltage of M1 causes M2 to reverse its transition toward cutoff. Although the current in M2 increases, the drain voltage decreases since it enters the strong inversion level. This effect is opposite to the previous one, causing the current and drain voltage of M1 to decrease. This mutual interaction between the transistors accounts for the ringing observed in the currents.

The duration of the ringing is influenced by internal and parasitic components. This current oscillation also affects the voltage waveforms, as shown in the figures.

Figure 4 brings the current waveform at the gate of M1. Neglecting the previously explained ringing, it is possible to see a sinusoidal shape in this current, compatible with the hypothesis that the voltage at drain is also a sinusoidal waveform. During the cutoff period, there is no current since the drain voltage is constant.

Figure 5 shows the current waveform in L1. One can see a sinusoidal waveform in the cutoff period of M1, again confirming that the voltage waveform at the drain is sinusoidal. During the conduction of M1, the current is a ramp, because of the integration of a constant voltage at the inductor.

Figure 6 shows the waveform of the current in the drain of M1. This transistor absorbs the current through the inductor when it is conducting. The current suffers an abrupt cutoff, as previewed by the theory. The on resistance (r_{on}) is so low that it is not possible to see any change in the drain to source voltage.

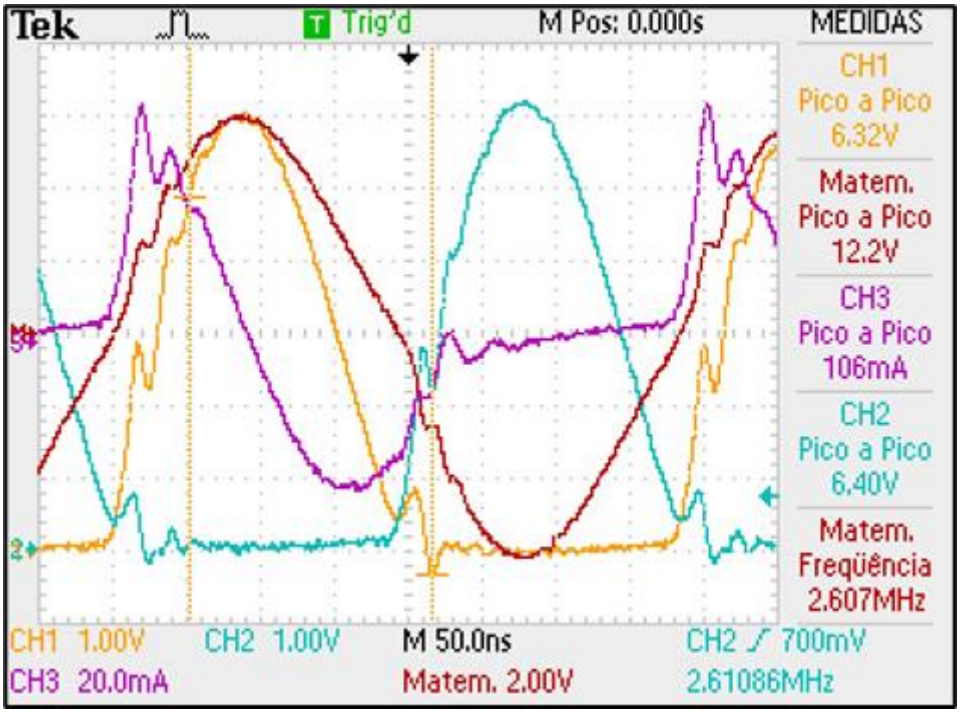

Figure 4. Waveforms at the oscillator. CH1: voltage at the drain of M1, CH2: voltage at the gate of M1, CH3: current at the gate of M1, Mathematic: differential voltage between the drains

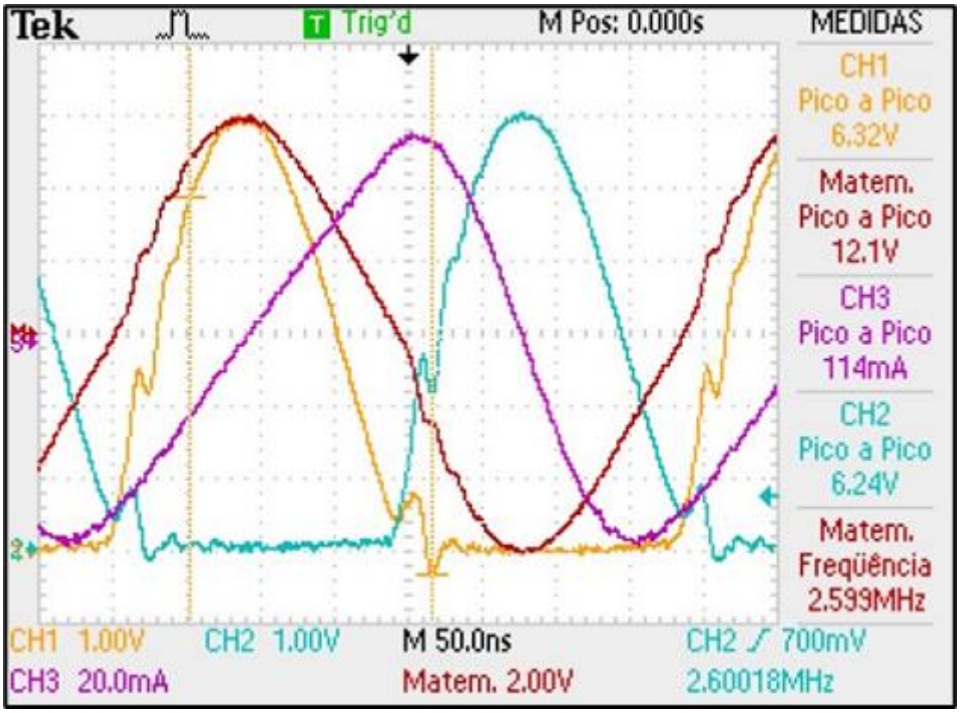

Figure 5. Waveforms at the oscillator. CH1: voltage at the drain of M1, CH2: voltage at the gate of M1, CH3: current at L1, Mathematic: differential voltage between the drains

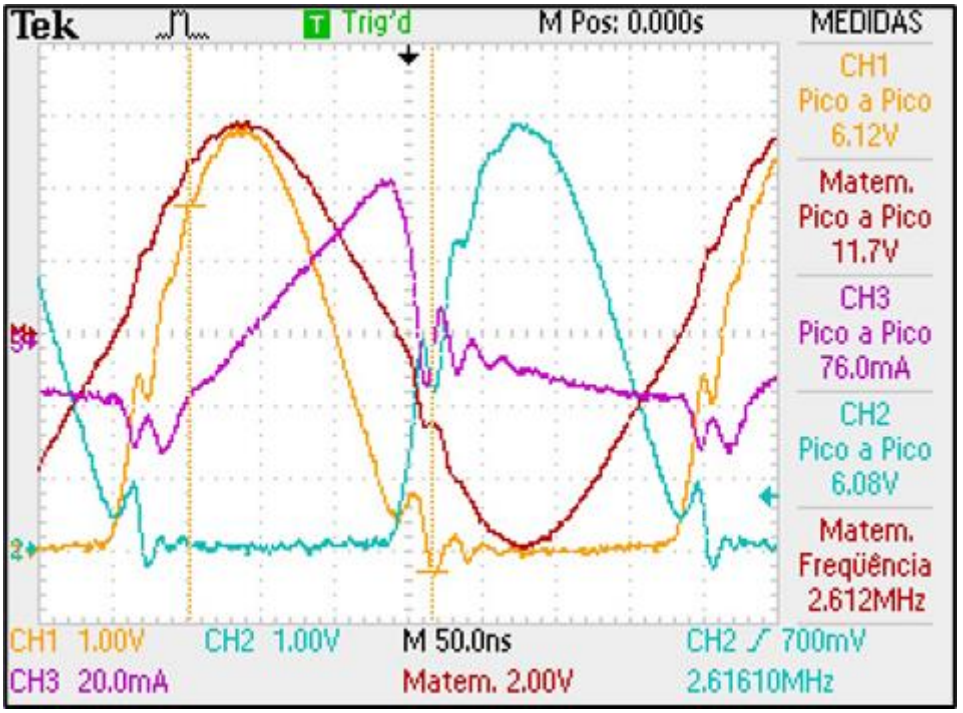

Figure 6. Waveforms at the oscillator. CH1: voltage at the drain of M1, CH2: voltage at the gate of M1, CH3: current at the drain of M1, Mathematic: differential voltage between the drains

In order to obtain T_F, it is necessary to find the period where v_0 nulls, which corresponds to $T_F/2$. Eq. (6) does not have an analytical solution, so a numerical one should be provided. Applying the values from the characterization of the circuit, the oscillation frequency $f_F = 1/T_F$ found by the software MATLAB is 2.650 MHz.

The MATLAB routine provided in Appendix A was used to obtain the theoretical waveform and theoretical parameters such as oscillation frequency and peak amplitude.

When compared to the experimental frequency (2.600 MHz), there is a deviation of 1.9 %. The experimental frequency lowers about 40 kHz/V with the increase of the power supply. This drift is caused by the decrease of the superposition period of the drain waveforms, which causes a slight variation in the period of oscillation. This effect is not predicted by the proposed theory, which defines a constant oscillation frequency. Figure 7 shows both curves as functions of the power supply.

Figure 8 illustrates the peak amplitude of the drain voltage as a function of the power supply. Theoretical values are about 37 % higher than the experimental ones. This can be explained by the transition of the transistors through the subthreshold region and by the fact that the voltage at the gate is not a voltage step, but a ramp. In addition, the transistors have a nonzero resistance. These effects lead the maximum current I_M to be lower than that predicted by the theory, since they delay and decrease the conduction of the transistor.

Figure 9 shows a comparison between the theoretical and experimental waveforms, normalized by the peak value of each waveform's data. They are very similar, showing that the approach represents the real behavior of the circuit.

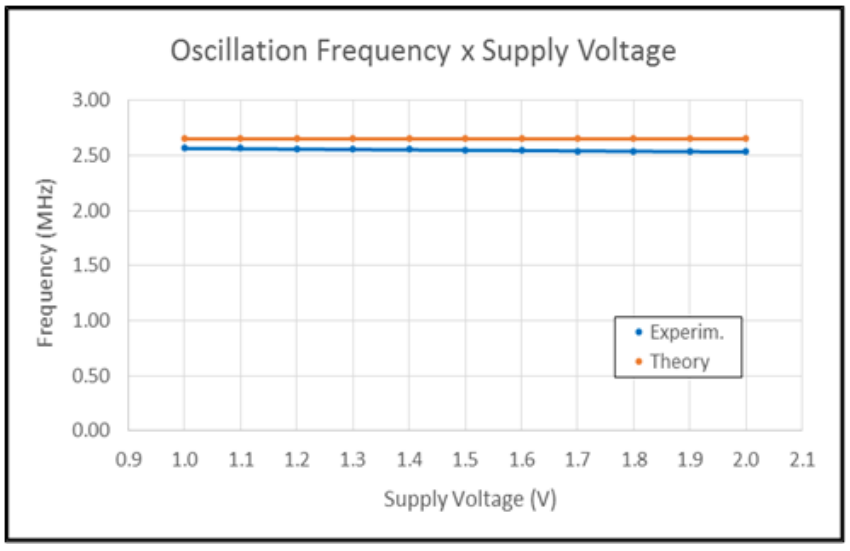

Figure 7. Theoretical and experimental oscillation frequencies as functions of the power supply

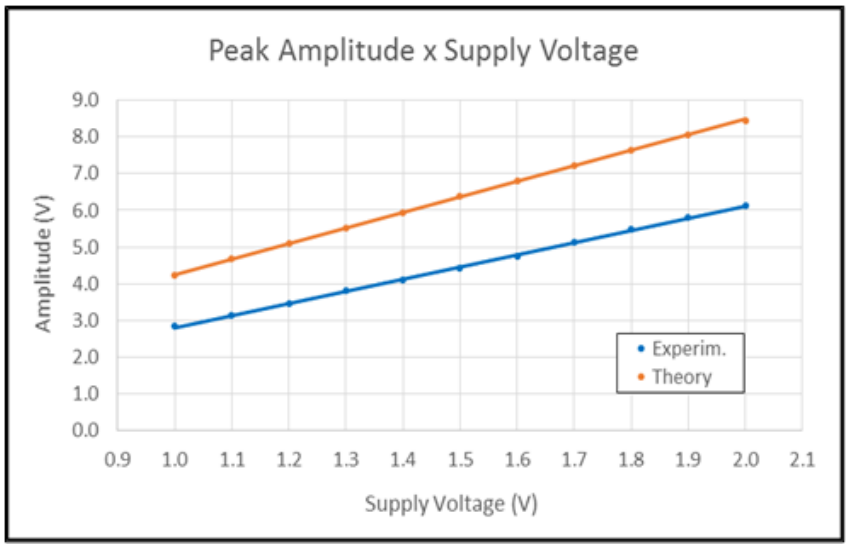

Figure 8. Theoretical and experimental peak amplitudes as functions of the power supply

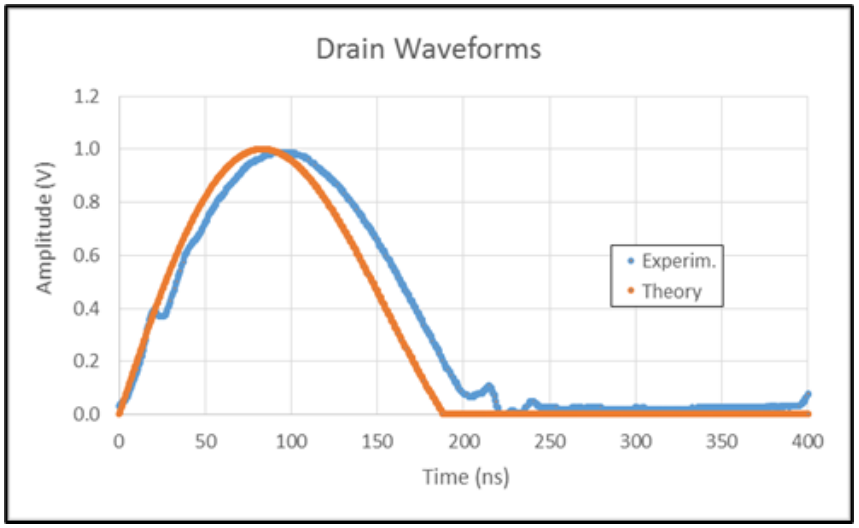

Figure 9. Drain waveforms, normalized by the peak value in order to show the similarity between the theoretical and experimental curves

5. Conclusions

A low-voltage cross-coupled oscillator was assembled and analyzed. An explanation to the working principle was presented. A preliminary model to the special case when transistors are considered as ideal switches was proposed.

The theoretical result in the oscillation frequency is quite close to the experimental one. In order to get a more faithful model for the peak amplitude, it is necessary to consider the complex relation between currents and voltages in the subthreshold region and the slower transition of the gate voltage. This is a topic for future research.

The modeling can be applied to circuits with different transistors and can accurately preview the oscillation frequency once the parasitic resistance and capacitance can be measured or predicted by design.

Acknowledgements

The authors would like to thank CNPq for the scholarship of R. G. Ono.

References

[1] M. Eshaghi and R. Rashidzadeh, “An energy harvesting solution for IoT sensors”, Proc. 2021 IEEE International Midwest Symposium on Circuits and Systems (September 2021).

[2] N. Garg and R. Garg, “Energy harvesting in IoT devices: A survey”, Proc. 2017 International Conference on Intelligent Sustainable Systems (June 2018).

[3] J. Rogers and C. Plett, Radio Frequency Integrated Circuit Design, Artech House, chap. 8, (2003).

[4] A. C. C. Telles, J. L. Emeri Jr. and S. Finco, “Demonstration of a low voltage power converter with application to photovoltaic cells”, Proc. X Workshop on Semiconductors and Micro & Nano Technology, (2015).

[5] A. Buonomo and A. Lo Schiavo, “Large-signal analysis of CMOS – LC VCOs”. IEEE ECCTD, pp. 994–997 (May 2007).

[6] A. Buonomo and A. Lo Schiavo, “Finding the tuning curve of a CMOS – LC VCO”, IEEE Trans. Circuits Syst. II, Express Briefs, vol. 55, no. 9, pp. 887–891, (September 2008).

[7] A. Buonomo and C. Di Bello, “Asymptotic formulas in nearly sinusoidal nonlinear oscillators”, IEEE Trans. Circ. Systems I: Fundamental Theory e Applications, vol. 43, no. 12, pp. 953-963, (December 1996).

[8] X. Ge, M. Arcak and K. N. Salama, “Nonlinear analysis of ring oscillator and cross-coupled oscillator circuits”, Dynamics of Continuous, Discrete and Impulsive Systems Series B: Applications and Algorithms [online]: http://hdl.handle.net/10754/247352.

[9] M. Daliri and M. Maymandi-Nejad, “Analytical model for CMOS cross-coupled LC-tank oscillator”, IET Circuits Devices Syst., pp. 1–9, (2013).

[10] M. B. Machado, M. C. Schneider and C. Galup-Montoro, “On the minimum supply voltage for MOSFET oscillators,” IEEE Trans. Circ. Systems I: Reg. Papers, vol. 62, no. 2, pp.347-357, (February 2014).

Appendix A

MATLAB routine to calculate the peak amplitude, oscillation frequency and the theoretical waveform’s data

```
% Define variable values:
% L: Average values of drain inductors
% C: Average value of gate capacitance
% R: Average value of gate resistance
% r: Resistance of drain inductors
% freq: Oscillation frequency

L = 3.3e-6;      % In Henry (H)
C = 731e-12;     % In Farad (F)
R = 18;          % In Ohms (Ω)
```

```
r = 0.3;              % In Ohms (Ω)

% Secondary modeling variables
sigmazero = ((R+r)/(2*L));
omegazero = 1/(sqrt(L*C));
omegad = sqrt((power(omegazero,2) - (power(sigmazero,2))));
r0 = sqrt((L/C) - (R*r));
thetad = atan((R-r)/(2*omegad*L));

% Time range for the curve
t = [0:0.4e-9:400e-9];

% FOR loop to obtain frequency values and peak value for each input voltage in v
% (2.0V to 1.0V)
for vdd = 2.0: -0.1: 1.0
% Define a function (fun) of one variable
(Tf)    fun=@(Tf)    vdd+(r0*((vdd*Tf)/(1*L*cos(atan(-((1/(omegad*Tf))+((R-r)/(2*omegad*L)))))))*(exp(-
sigmazero*Tf))*(sin((omegad*Tf) + (atan(-((1/(omegad*Tf))+((R-r)/(2*omegad*L)))))+ (thetad))));

% For each FOR loop iteration, the 'fzero' function is used to find the value of 'Tf' where 'fun(Tf) = 0'.
This search is done between 180ns and 220ns
Tf = fzero(fun,[180e-9 220e-9]);

% For each FOR loop interaction, the values of the variables below are updated as they depend on
'Tf'
thetai = atan(-((1/(omegad*Tf))+((R-r)/(2*omegad*L)))); im = (vdd*Tf)/(L);
i0 = im/(cos(thetai));

% Calculate the curve voltages
v0 = vdd + (r0*i0*(exp(-sigmazero*t)).*(sin((omegad*t) + thetai + thetad)));

% Find the maximum value of the voltage v0
K = max(v0);

% Calculate the oscillator frequency for each supply voltage
freq = 1/(2*Tf);

% Transpose the v0 vector to facilitate data transfer to Excel
v2 = v0';

end
```